Development and Evaluation of Two New Droplet Evaporation Schemes for Fire Dynamics Simulations

JASON FLOYD[1], RANDALL MCDERMOTT[2]
[1]JENSEN HUGHES, Rockville, Maryland, USA
[2]National Institute of Standards and Technology, Gaithersburg, Maryland, USA

ABSTRACT

The evaporation of sprinkler droplets is an important phenomena in fire simulations both for heat removal from the gas and for heat removal from surfaces. The Fire Dynamics Simulator (FDS) has seen a number of different evaporation models over its history where each subsequent model has attempted to address limitations and issues with the previous model. In this paper, we address the problems of potential numerical instability and super-saturation that may occur in explicit time integration of the droplet equations. Two novel numerical approaches are developed and evaluated. The first is based on an analytical solution that relaxes the cell composition and temperature toward the equilibrium values. The second method is an implicit solution to the droplet equations. The two approaches are verified and validated using both single droplet and practical sprinkler calculations. Ultimately, the implicit approach is demed the most cost effective for practical fire simulations.

KEYWORDS: FDS, large-eddy simulation, evaporation, sprinklers

NOMENCLATURE

A	surface area (m^2), computational time (s)
B, C	computational time per droplet (s/droplet)
c	heat capacity (J/kg/K)
F, G	droplet temperature solution components
H	enthalpy (J)
h	heat transfer coefficient ($W/m^2/K$)
h_l	liquid enthalpy (J/kg)
h_m	mass transfer coefficient (m/s)
h_v	heat of vaporization (J/kg)
M	total normalized vaporization rate (1/s)
N	number of particles per cell
m	droplet mass (kg)
$\dot{q}_r$	droplet radiation absorption (W)
t	time (s)
T	droplet temperature (K)
T_g	gas temperature (K)
T_w	wall temperature (K)
Y	vapor mass fraction (kg/kg)
V	cell volume (m^3)

Greek

β	analytical solution parameter ($kg^{1/3}/s$)
$\delta\hat{t}$	small time step (s)
Δt	time step size (s)
ρ	gas density (kg/m^3)
χ	area per mass factor ($m^2/kg^{2/3}$)
ω	relaxation time constant (1/s)

superscripts

n	time step

subscripts

eq	cell equilibrium condition
f	film
g	gas
i	droplet index
l	liquid at equilibrium
m	mass transfer
v	vapor, vaporization
w	wall

INTRODUCTION

The evaporation of sprinkler droplets is an important phenomena to consider when modeling the thermal environment due to a fire. For standard large drop sprinklers (e.g. not a watermist system), efficacy of droplets have been estimated analytically [1] and confirmed experimentally [2] to remove between 11 % and 26 % of the heat produced by a fire. Watermist systems can remove 100 % of the heat produced by a fire either by extinguishment or by providing sufficient evaporation to maintain compartment temperatures at or below the boiling point of water [3].

A successful model of droplet evaporation in fire dynamics simulations should

(1) accurately represent droplet dynamics

(2) conserve mass and energy

(3) be computationally efficient

(4) be numerically stable

(5) obtain the correct equilibrium state

(6) be independent of the order in which the droplets are processed

Typical computational fluid dynamics (CFD) codes use either stiff explicit or segregated implicit ODE time integrators to solve the droplet dynamics equations. These solvers, in general, satisfactorily address the issues of accuracy and conservation (Items 1 and 2).

To address computational efficiency (Item 3) CFD codes do not track every droplet from a sprinkler—the cost would be too high. Instead, a smaller number of "superdroplets", where each superdroplet represents multiple individual droplets. This approach, while cost effective, can lead to extremely high rates of heat and mass transfer when very fine droplets require a large superdroplet weighting factor. These high heat and mass transfer rates present significant numerical challenges for computational efficiency and numerical stability (Item 4). The methods presented in this paper are aimed at addressing these two critical, practical issues in droplet evaporation for fire modeling applications.

The methods discussed in this work also address equilibrium (Item 5) and droplet order (Item 6) more directly than in the past. These are subtle issues that are discussed in more detail later in the paper.

The NIST Fire Dynamics Simulator (FDS) [4, 5] has seen a number of approaches to droplet evaporation in an attempt to achieve the desirable model attributes listed above. A brief history is summarized below:

FDS 1-4 used an explicit solver for the heating and evaporation of droplets. During this time period, development of routines for droplet transport and evaporation focused on applications like the sprinkler suppression of commodity using a simple exponential decay of the heat release rate based on the delivered quantity of water [6].

FDS 5 came with a significant overhaul to the droplet model. This in large part resulted from efforts to model water mist systems where the approach taken in FDS 1-4 resulted in numerical instabilities. In a water mist system, especially upon initial discharge, very large changes in droplet temperature and gas temperature can occur. The explicit approach being used could result in large, non-physical swings in gas and droplet temperature leading to numerical instabilities. The droplet model was changed to a semi-implicit method where the droplet mass and temperature were solved implicitly and the gas temperature (and wall temperature for a droplet on a solid surface) was solved explicitly. This approach resolved many of the issues with numerical instabilities. As more rigorous verification and validation practices became used in FDS development, this semi implicit approach underwent further modifications to ensure the conservation of energy.

FDS 6 introduced some additional changes to the droplet model. Most notably, a self-consistent set of thermophysical properties was introduced for common species using NIST-JANAF data [7]. This effort ensured the correct equilibrium state was being reached. Users of FDS continued trying to expand its application space with applications including very fine water mist (fog) and sprinkler suppression of pyrolyzing materials. The new routine had difficulties with these two classes of problems: droplets impacting hot surfaces with low conductivity and low thermal inertia (for example foams) and simulations with very fine water mist. The root cause in both cases was that the explicit solver being used for the gas and wall temperatures was resulting in large overshoots or undershoots in temperature prediction. This resulted in anomalous temperatures in the simulation or runtime failures when bad temperature values were used in other subroutines.

DEVELOPMENT OF NEW EVAPORATION SCHEMES

In this work, two new schemes are developed and evaluated to address the shortcomings of other methods discussed above. The first is a relaxation method based on an analytical solution to an alternate set of droplet equations. The second is an implicit, drop-wise approach (which we ultimately determine to be superior in terms of computational cost and ease of implementation). Below we present the governing equations followed by an overview of the new schemes. Details are provided in Appendices A and B.

Governing Equations

The governing equations for droplet evaporation are given below and may be found in Ref. [8]. Summations are over all droplets in a computational cell. Again, note that each individual droplet represents a superdroplet with a mass weighting factor (omitted here to avoid complicating the equations). Details may be found in [4].

$$\frac{\mathrm{d}m_i}{\mathrm{d}t} = A_i h_{m,i} \rho \left(Y_v - Y_{l,i}\right) \tag{1}$$

$$\rho V \frac{\mathrm{d}Y_v}{\mathrm{d}t} = -\sum_i \frac{\mathrm{d}m_i}{\mathrm{d}t} \tag{2}$$

$$m_i c_i \frac{\mathrm{d}T_i}{\mathrm{d}t} = A_g h_g \left(T_g - T_i\right) + A_w h_w \left(T_w - T_i\right) + \frac{\mathrm{d}m_i}{\mathrm{d}t} h_v + \dot{q}_r \tag{3}$$

$$m_g c_g \frac{\mathrm{d}T_g}{\mathrm{d}t} = -\sum_i \left(A_g h_g \left(T_g - T_i\right) + \frac{\mathrm{d}m_i}{\mathrm{d}t} \left(h_v + h_l\right) \right) \tag{4}$$

$$m_w c_w \frac{\mathrm{d}T_w}{\mathrm{d}t} = -\sum_i A_w h_w \left(T_w - T_i\right) \tag{5}$$

Equation (1) defines the droplet evaporation as a function of the droplet surface area, A_i and a mass transfer coefficient, $h_{m,i}$, times the difference in the gas vapor fraction, Y_v, and the droplet surface vapor fraction, $Y_{l,i}$, evaluated using the Clausius-Clapeyron equation.

Equation (2) defines the rate of change in vapor mass in a gas cell as the sum of the evaporation rates of the droplets in the cell.

Equation (3) defines the rate of change in the droplet temperature, T_i. This consists of two convective terms, an evaporation term, and a radiation absorption term. The first convective term is for heat transfer to the gas based on the droplet area exposed to the gas, A_g, and a gas heat transfer coefficient, h_g. The second convective term is for heat transfer to the wall based on the droplet area exposed to the wall, A_w, and a wall heat transfer coefficient, h_w. The third term accounts for energy lost due to the heat of vaporization, h_v. The fourth term, $\dot{q}_r$, represents the radiative energy absorbed by the droplet.

Equation (4) defines the rate of change in the gas temperature, T_g. It sums the heat transfer from the droplet plus the enthalpy of evaporated mass over all droplets in the cell.

Equation (5) defines the rate of change in the wall temperature, T_w. It sums the heat transfer from the droplet over all droplets on the wall cell.

Note that fluid properties used for determination of the heat and mass transfer coefficients (conductivity, diffusivity, viscosity) are evaluated at the droplet film temperature, $T_{f,i}$, using the one-third rule, as discussed in [9]:

$$T_{f,i} = T_i + \left(T_g - T_i\right)/3 \tag{6}$$

Heat of vaporization is evaluated at the droplet surface temperature, which is the same as the droplet temperature in the thermally thin limit considered here.

Relaxation-to-Equilibrium Method

The relaxation-to-equilibrium method (hereafter "relaxation" method) presented in this paper is a novel numerical approach to a class of transient problems where an equilibrium state can be readily established but where an equilibrium solution may not be desirable. Such problems include drag, chemical kinetics, and evaporation. In general, one does not know *a priori* whether the time step dictated by other physics in the

problem will require a time accurate solution or an equilibrium solution. In the case where the correct solution is equilibrium, it does not make sense to waste time marching toward the solution with an explicit integration technique. The alternative of using a fully implicit, nonlinear solution method can also be complex and expensive. The method we present here has some of the advantages of a fully explicit approach and some advantages of the implicit approach. We are able to obtain a time accurate solution for small time steps and a stable equilibrium solution in one large quasi-explicit time step. The details of the scheme are provided in Appendix A.

As we discuss below, evaluation of the exponentials and logarithms inherent in the analytical solution significantly hinder its performance compared to the other method we will discuss in this paper, a novel semi-implicit formulation. We stress that this conclusion is problem dependent. But for the practical engineering problems considered here, the relaxation method is more expensive than the semi-implicit scheme. Therefore, ultimately, the semi-implicit approach will become the default in future versions of FDS. The development and results of the relaxation method are still retained in this paper, however, since the method is novel and may be useful in other fire science problems.

Implicit Method

It was postulated that the numerical issues in the droplet routine could be due to inconsistencies between the explicit update of the gas and wall temperatures and the implicit determination of the droplet evaporation rate. To remedy this problem, we developed and implemented a method where the dependent variables are treated implicitly, while other quantities are linearized using their initial values. Implicit solutions for Y_v, T_i, and T_g (and the wall temperature T_w, if necessary) are developed in Appendix B.

The equations are solved on a droplet-by-droplet basis. Thus, if the number of droplets in a cell is greater than one the initial conditions for Y_v, T_g, and T_i for a given droplet are taken from the result of the integration from the previous droplet. The order in which the droplets are processed is not set explicitly. Rather, in a typical fire application the chaotic path of the droplets combined with their initial numerical ordering (during the droplet injection step) lead to a quasi-random droplet order for a given cell during the evaporation time integration. In a typical engineering calculation, it would be rare for more than one droplet to be in a cell.

RESULTS AND DISCUSSION

Verification and Validation

This section presents the results of a series of verification and validation cases. Verification is the process of demonstrating that a model implementation accurately represents its conceptual framework (are the equations being solved correctly) and validation is the process of demonstrating that a model, based on its intended use, makes reasonable predictions of the real world [10]. The cases are from the FDS verification suite [11]. The FDS verification suite contains eight cases testing droplet evaporation. Five of the eight cases are shown below to highlight the performance (in terms of the model properties listed above) of the current version (FDS 6.5.3 at the time of the writing), which will be referred to as the "explicit" approach, compared against the relaxation and implicit approaches. The cases that follow test mass and energy conservation, the end equilibrium state, and the prediction of the evaporation rate.

Case 1: Complete Evaporation of Monodisperse Droplets

The geometry for this case (*water_evaporation_1* in the FDS verification suite), is a 1 m^3 box with adiabatic walls uniformly gridded with 10 cm cells. The initial conditions in the box are 200 °C air at 0 % humidity. The box is uniformly seeded (10 droplets per cell) with 0.01 kg of static droplets at 20 °C and a uniform diameter of 200 μm. Since the droplets are cooler than the air and the air has no water vapor, a non-equilibrium condition exists. Equilibrium will be achieved at a point where the droplet temperature equals the gas temperature and vapor mass fraction in the gas equals the droplet equilibrium vapor fraction. The equilibrium condition can be determined analytically using the thermophysical properties of air and water. The approach is to first determine the initial total enthalpy present (i.e., the sum of the droplet and gas enthalpies). Then a new temperature is selected, the equilibrium vapor fraction for that temperature computed, liquid evaporated to meet the equilibrium vapor condition, and the total enthalpy computed (accounting for pressure work

in a sealed domain) and compared to the initial enthalpy. This process is repeated until the final enthalpy equals the initial enthalpy. For Case 1, the equilibrium condition results in all the water evaporating. Table 1 shows the expected results and the results computed by the explicit, equilibrium, and implicit methods. All evaporation methods predict the expected values with only minor errors.

Table 1. Results of Verification Case 1: Complete Evaporation of Monodisperse Droplets

Variable	Expected Value	Explicit	Relaxation	Implicit
Relative Humidity (%)	2.1	2.1	2.1	2.1
Change in gas enthalpy (kJ)	-167	-166	-166	-166
Change in water enthalpy (kJ)	159	159	159	159
Change in pressure (Pa)	7810	7800	7790	7801
Final temperature (°C)	154	154	154	154

Case 2: Steady State Evaporation in Hot Channel Flow

The geometry for this case (FDS *water_evaporation_4*), is a 3 m $\times$ 1 m $\times$ 1 m tunnel. One end of the tunnel is open, the other end has an inlet condition of 500 °C air at 1 m/s and 0 % humidity, and the remaining walls are adiabatic. After a brief period to allow the flow field to develop, static droplets are injected into the tunnel at a rate of 0.05 kg/s and a temperature of 20 °C with a uniform diameter of 20 μm. There is sufficient excess energy over the boiling point of water in the inflowing air to fully evaporate the mass of droplets being injected. Using the thermophysical properties of air, one can compute the enthalpy flow of the incoming air and the enthalpy flow of the outgoing air, which now contains water vapor. Table 2 shows the expected results and the results computed by the explicit and the implicit methods (note, based on timing results shown later in the paper, the equilibrium method was not developed to the point of being able to run this case). Both the explicit and the implicit methods predict the expected values with only minor errors.

Table 2. Results of Verification Case 2: Steady State Evaporation in Hot Channel Flow

Variable	Expected Value	Explicit	Implicit
Heat flow prior to droplets (kW)	230	229	229
Heat flow after droplets (kW)	107	107	107

Cases 3: Single Droplet Rate of Evaporation (Verification)

Case 3 (FDS *water_evaporation_8*) compares the FDS time accurate solution against the evaporation model of [9]. The simulation consists of an injection of a 100 μm droplet at 10 °C into 60 °C air with an initial water vapor mass fraction of 10 %. Results are shown below in Fig. 1(left). With a sufficiently small time step, here $\Delta t = 0.001$ s, all three numerical methods produce the same results, which is to be expected for convergent schemes. Minor differences between FDS and the Li & Chow numerical solution are attributable to small differences in fluid properties, drag formulations, and the fact that the Li & Chow solution is effectively zero dimensional (solution of ODEs), whereas the FDS solution is, of course, integrated in a CFD solver.

Cases 4: Single Droplet Rate of Evaporation (Validation)

Case 4 (FDS *water_evaporation_5*) evaporates a single 1 mm droplet initially at 9 °C in 25 °C air. The expected results are from experimental test data [12] where a single droplet was suspended on a glass fiber. Results are shown in Fig. 1(right). Again, the numerical methods all produce the same result for the same problem. Note that here care has been taken to ensure that fluid properties for the explicit results have been evaluated in exactly the same manner as for the relaxation and implicit methods.

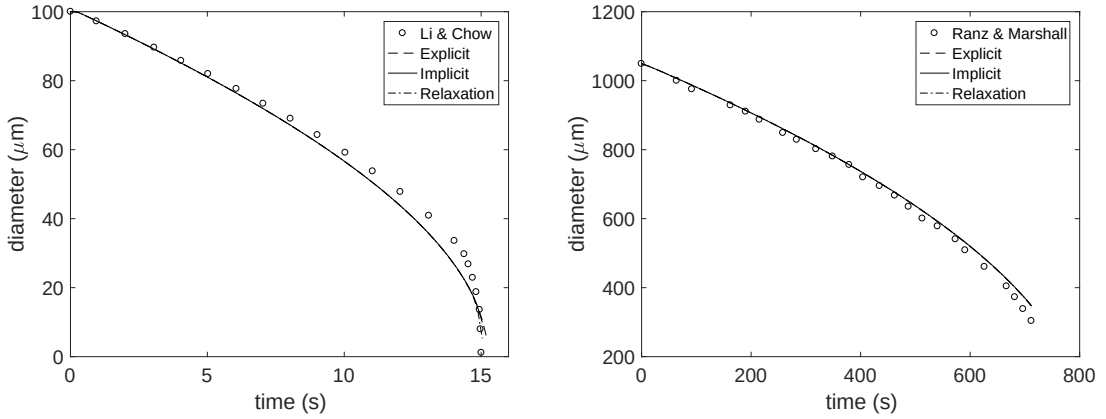

Fig. 1. (Left) Case 3: Single droplet verification with drag. Comparison with numerical solution of Li and Chow [9]. (Right) Case 4: Single droplet validation in quiescent air. Comparison with experimental data of Ranz and Marshall [12].

Case 5: Energy Conservation in Droplet-Wall Interaction

This case (FDS *water_evaporation_6*) extends the complete evaporation case to include heat transfer to walls. The geometry for the case is a 1 m^3 box with adiabatic walls and an adiabatic ceiling. The floor is a plate with an insulated back that is 1 mm thick with a density of 1000 kg/m^3, a heat capacity of 1 kJ/(kg·K), and an initial temperature of 250 °C. The initial condition in the box is 100 °C air and 0.1 kg of water droplets with an initial temperature of 20 °C and an initial diameter of 2 mm. The droplets are defined as a liquid with a heat capacity of 2 kJ/(kg·K), a boiling point of 100 °C, a density of 1000 kg/m^3, and a heat of vaporization at the boiling point of 173.15 kJ/kg. Following the procedure outlined in Case 1, the final state can be computed using the solid, liquid, and gas thermophysical properties. Table 3 shows the expected results and the results computed by the explicit and the implicit evaporation methods (note, based on timing results shown later in the paper, the equilibrium method was not developed to the point of being able to run this case). Both methods predict the expected values with only minor errors.

Table 3. Results of Verification Case 4: Energy Conservation in Droplet-Wall Interaction

Variable	Expected Value	Explicit	Implicit
Change in pressure (Pa)	34600	34500	34500
Final gas temperature (°C)	172	172	172
Final wall temperature (°C)	172	172	172

Algorithm Cost

Given the suitable and comparable results of the two schemes, computational cost becomes the criterion for acceptance of the method. Below we discuss the computational complexity.

Execution time t for the relaxation and the implicit methods, respectively, can be characterized as

$$t = A + B \times N \tag{7}$$

$$t = C \times N \tag{8}$$

where N is number of droplets per cell and A, B, and C are constants. A is the time to find the equilibrium solution once droplet masses and enthalpies have been determined in the gas cell. Initially, it was thought that this cost might limit the performance of the relaxation method. B is the cost in the relaxation method to sum the mass and enthalpy of a single droplet in a gas cell plus the time to update the droplet mass and temperature once the equilibrium condition is known. C is the cost to update one droplet with the semi-implicit method.

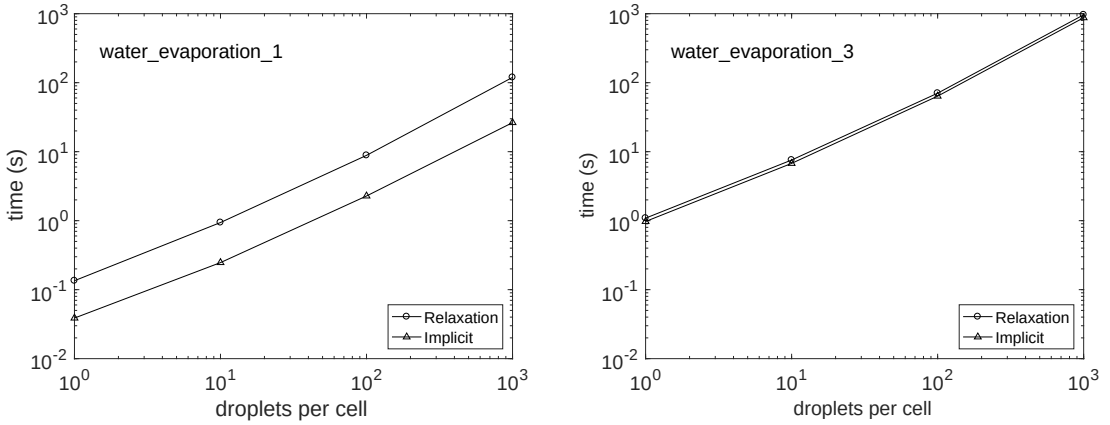

Fig. 2. Results of the algorithm cost for various numbers of particles per cell for complete evaporation (left, Evaporation 1) and partial evaporation (right, Evaporation 3) of monodisperse droplets.

The assumption underlying the development of the relaxation model was that $C > B$ and that for some small number of droplets per cell the analytical solution would be cheaper than the implicit approach. Note that for $C > B$ the cost of relaxation is less than implicit when

$$N > A/(C-B) \tag{9}$$

However, if $C < B$ then, by definition, implicit is always cheaper.

The relative costs, C and B, are determined using two sets of simulations. The first uses Case 1 from above. The second uses a similar case which increases the initial gas temperature to 500 °C and increases the initial droplet diameter to 200 μm. In this second case the droplets do not fully evaporate. Each case is run with a varying number of droplets per cell. The results are shown in Fig. 2. As seen, the relaxation model is always more costly, even for a large number of droplets per cell. In the complete evaporation case (left, Evaporation 1) relaxation is significantly more expensive. It must be concluded, therefore, that $C < B$ for the current implementation. We attribute this result to the significant number of exponential and logarithmic operations needed to evaluate the analytical solution for the relaxation scheme. Contrary to our original assumptions, it appears that evaluation of the equilibrium state is reasonably efficient. Therefore, the relaxation scheme may yet be useful. The present results, however, have led to the adoption of the implicit method going forward.

Test of Expanded Application Space

The prior section demonstrates that the proposed implicit method conserves mass and energy, makes reasonable predictions of the evaporation rate, obtains the correct equilibrium end state, and avoids significant computational cost. The explicit method performed similarly for these simple tests. This section of the paper demonstrates that the new, implicit method overcomes limitations of the explicit method routine and expands the application space of the evaporation model.

As previously discussed, the explicit evaporation model does not directly couple the gas and wall temperature to the droplet temperature solution. This can result in non-physical changes in gas and wall temperature under some conditions. For example, consider a cold superdroplet (representing many real droplets) hitting a hot wall with a very low thermal inertia. Without an implicit wall temperature update in the evaporation model, the heat transfer to the wall will be significantly over predicted for typical FDS time steps. In the wall heat transfer routine, that heat transfer imposed as a boundary condition could result in a very large drop in surface temperature. Similarly for the gas temperature, consider very small droplets not at thermal equilibrium with the gas. The high surface area to volume ratio of small drops can lead to over predictions of heat transfer with the gas when the gas temperature is not treated implicitly. The result can be non-physical changes in the cell gas temperature.

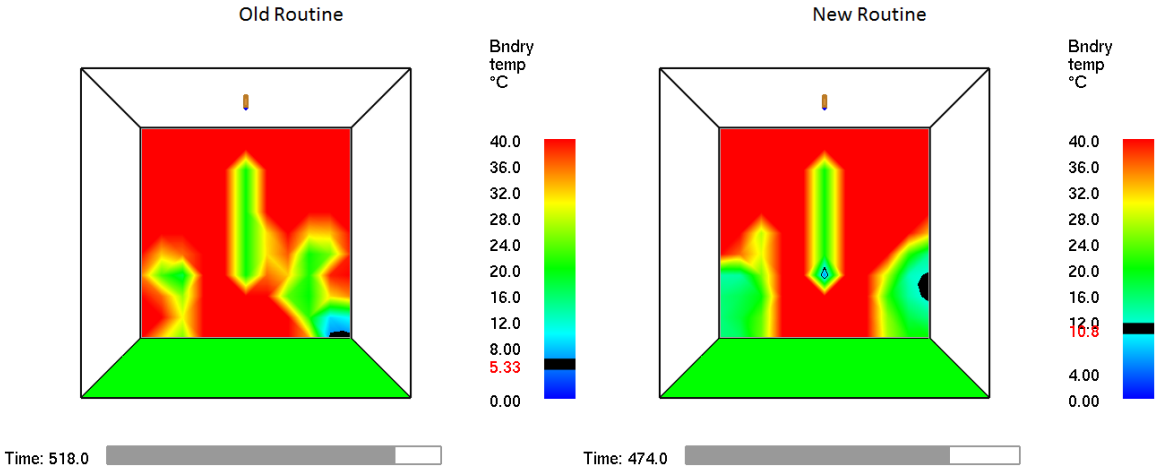

Fig. 3. Wall temperatures resulting from droplets on a burning, low density, low thermal conductivity surface (Left - Explicit, Right - Implicit). Black highlighted contour is lowest temperature.

Cold Spray on Hot Insulated Walls

In this example, a geometry is defined that consists of a burner against a wall made of a combustible, low density, low thermal conductivity material. The burner is allowed to ignite the material, and after a brief period of fire spread, a sprinkler is operated. With the explicit method, this test case is unsuccessful. The low density and low thermal conductivity of the material results in a very small amount of mass in the first wall cell node. Shortly after sprinkler operation, overshoots in the prediction of the wall temperature result in excessive heat removal that eventually leads to a wall cell reaching a 0 K surface temperature, and FDS aborting its calculation.

The new implicit routine couples the wall cell surface temperature to the droplet temperature computation. This limits the amount of heat transfered from the hot wall to the cold droplets on its surface. The result is that very large temperature decreases are avoided and the simulation is stable. Note that presently the implicit method is not fully coupled with the 1D solid phase heat transfer solver (which would be costly), so lower than expected temperatures do occur but not at the magnitude seen with the explicit method. While the exact moment of the failure is not captured in the output files, Fig. 3 shows the output interval for each simulation that had the lowest observed temperatures. The figure shows the wall temperatures for the explicit method on the left and for the implicit method on the right. For each simulation the contour highlighting the lowest temperature at that time is displayed as a black contour with the value in the color bar in red text. As seen the implicit method does not show the very low temperatures seen with the explicit method. The new routine also avoids the numerical error and allows the simulation to complete successfully.

Injection of Very Fine Mist

This example demonstrates an application where very fine water mist is injected. The simulation consists of a 5 m $\times$ 5 m $\times$ 10 m box at 30 °C with a water mist nozzle at mid-height. The nozzle injects a very fine mist of 50 μm at 10 °C. In the explicit method, with the droplet temperature decoupled from the gas temperature, there is an overshoot in heat transfer from the gas to the droplets near the nozzle, resulting in droplet temperatures in excess of 75 °C. Investigation of this scenario determined that the very small droplets had a very high evaporation rate and heat transfer rate. Since the gas temperature was not being solved implicitly together with the droplet temperature, some droplets initially overshot the gas temperature. Those (now hot) droplets then convected the heat back to the gas resulting in elevated gas temperatures in some regions. In the implicit method, the simultaneous solution of the gas and droplet temperature prevents the droplets from overshooting the gas temperature as they heat up. The result is no droplets see temperatures over the initial gas temperature. This is shown below in Fig. 4 which shows droplets colored by temperature shortly after the spray injection starts. With the old routine some droplets were heating to over 80 °C and

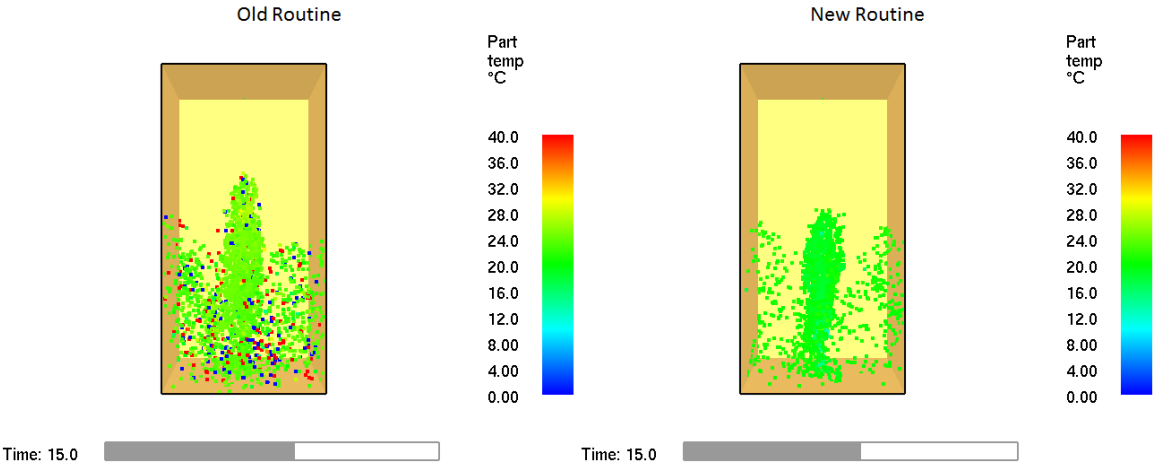

Fig. 4. Injection of very fine, cold water mist into air (left - Explicit, right - Implicit).

some were cooling to freezing (0 °C). In the new routine droplets do not exceed 22 °C, a more reasonable value given an initial gas temperature of 30 °C.

CONCLUSIONS

Droplet evaporation capabilities have seen a continuous evolution since the release of FDS 1 in response to user desires to expand the application space of FDS. This paper continues that evolution by deriving two new approaches for solving the droplet heat and mass transfer equations since explicit approaches for evaporation do not perform well under conditions of very small droplets or cold droplets on hot surfaces with low thermal inertia. The first approach is a novel relaxation-to-equilibrium method, which is applicable to a range of problems requiring time accuracy and stability, such as drag, chemical kinetics, and evaporation. While successful in correctly predicting equilibrium conditions and droplet evaporation rates, the relaxation method proved to be costly for the engineering applications chosen for this study. This led to the development of the second approach, a semi-implicit solution to the governing equations for a single droplet.

The implicit approach has been implemented in FDS and tested against a range of verification and validation problems. The approach was also tested against problems where the explicit method did not perform well. Results demonstrate that the implicit approach conserves mass and energy, and correctly predicts equilibrium without a significant change in computational cost.

REFERENCES

[1] W.K. Chow. On the evaporation effect of sprinkler water spray. *Fire Technology*, 25:364–372, 1989. doi: http://dx.doi.org/10.1007/BF01040382.

[2] S.C. Li, D. Yang, L.H. Huo, Y.Z Li, and H.B. Wang. Studies of cooling effects of sprinkler spray on smoke layer. In *Fire Safety Science – Proceedings of the Ninth International Symposium*, pages 861–872. International Association of Fire Safety Science, 2008. doi: http://dx.doi.org/10.3801/IAFSS.FSS.9-861.

[3] G.G Back, C.L. Beyler, P.J. DiNenno, R. Hansen, and R. Zalosh. Full-scale testing of water mist fire suppression systems in machinery spaces. CG-D-26-98, United States Coast Guard, Washington, DC, 1998.

[4] K. McGrattan, S. Hostikka, R. McDermott, J. Floyd, C. Weinschenk, and K. Overholt. Fire Dynamics Simulator Technical Reference Guide Volume 1: Mathematical Model. NIST SP 1018-1, National Institute of Standards and Technology, Gaithersburg, MD, 2016.

[5] K. McGrattan, S. Hostikka, R. McDermott, J. Floyd, C. Weinschenk, and K. Overholt. Fire Dynamics Simulator User's Guide. NIST SP 1019, National Institute of Standards and Technology, Gaithersburg, MD, 2016.

[6] A. Hamins and K. McGrattan. Reduced-scale experiments to characterize the suppression of rack storage commodity fires. NISTIR 6439, National Institute of Standards and Technology, Gaithersburg, MD, 1999.

[7] M.W. Chase, C.A. Davies, and et al. NIST JANAF Thermochemical Tables 1985 Version 1. NIST SRD 13, National Institute of Standards and Technology, Gaithersburg, MD, 1986.

[8] N. Cheremisinoff. *Encyclopedia of Fluid Mechanics, Volume 3: Gas-Liquid Flows*. Gulf Publishing Company, Houston, TX, 1986.

[9] Y.F. Li. and W.K. Chow. Study of water droplet behavior in hot air layer in fire extinguishment. *Fire Technology*, 44:351–381, 2008. doi: http://dx.doi.org/10.1007/s10694-007-0036-2.

[10] A.B. Carter. DoD Modeling and Simulation (M&S) Verification, Validation, and Accreditation (VV&A). DOD 5000.61, United States Department of Defense, Washington, DC, December .

[11] K. McGrattan, S. Hostikka, R. McDermott, J. Floyd, C. Weinschenk, and K. Overholt. Fire Dynamics Simulator Technical Reference Guide Volume 2: Verification. NIST SP 1019, National Institute of Standards and Technology, Gaithersburg, MD, 2016.

[12] W.E. Ranz and R. Marshall. Evaporation from droplets. *Chemical Engineering Progress*, 48:141–146, 1952.

A Development of a Stable Relaxation Solution

In this appendix, we present a solution method based on relaxation to the "equilibrium state" of a given computational cell. The scheme uses a forward Euler solution at extremely small time steps for the initial relaxation rate, ensuring convergence. Stability is guaranteed for large time steps because we solve the governing equations analytically. As a result, the scheme is first-order accurate and never over-shoots the saturation condition.

Our goal is to design a single step scheme which does not over-shoot the saturation condition. The equilibrium state of the droplet mass and temperature are determined by the cell pressure, composition, and the enthalpy. Then, as if we were looking up the result in a steam table, we establish the equilibrium droplet temperature and droplet mass, the values which would be obtained if the rate equations were integrated to time equals infinity.

The enthalpy of the cell is given by

$$H = \sum_i m_i c_{p,l}(T_i) T_i + m_g \bar{c}_{p,g}(\mathbf{Y}, T_g) T_g \tag{10}$$

$$= \sum_i (m_i - \delta m_i) c_{p,l}(T_{eq}) T_{eq} + (m_g + \delta m) \bar{c}_{p,g}(\mathbf{Y}, T_{eq}) T_{eq} - \dot{q}_r \tag{11}$$

where $\delta m = \sum_i \delta m_i$ is the total mass evaporated at equilibrium conditions. The specific heat of the gas, $\bar{c}_{p,g}$, is tabulated as a function of temperature and composition and includes the heat of vaporization.

Note that *equilibrium* does not imply *saturation*. The cell equilibrium is the resulting state of gas phase composition, temperature, and quality (vapor fraction) under adiabatic conditions. There are two situations

to consider at equilibirum: (1) all water evaporates (under-saturated) and (2) only a fraction of the water evaporates (saturated). Details of the algorithm to determine this state are omitted here for brevity.

The method we have developed to integrate the evaporation model is called a *relaxation scheme*. It takes advantage of two known facts:

(1) An explicit update to Eqs. (1) through (5) is stable and accurate for some small time step.

(2) The equilibrium solution should be obtained for large time steps.

The strategy is to recast the ODEs into a form with a simple analytical solution that is consistent with the facts just stated.

The ODE for the gas phase vapor fraction from Eq. (2) is

$$\rho V \frac{\mathrm{d}Y_v}{\mathrm{d}t} = -\sum_i \frac{\mathrm{d}m_i}{\mathrm{d}t} = -\rho \sum_i A_i h_{m,i}(Y_v - Y_{l,i}) \tag{12}$$

This equation is recast into the form

$$\frac{\mathrm{d}Y_v}{\mathrm{d}t} = -\omega (Y_v - Y_{eq}) \tag{13}$$

which has the simple solution

$$Y_v(t) = Y_{eq} + (Y_{v,0} - Y_{eq}) \exp(-\omega t) \tag{14}$$

It remains that we find a value for the time constant ω such that the solution (14) closely approximates the solution to (12) for small time steps. It is guaranteed that $Y_v = Y_{eq}$ for large time steps. The error for anything in between is impossible to access given the myriad of assumptions underlying the model, and we should be happy with a smooth transition between the two extremes.

The time constant ω is obtained by equating the solutions to a forward Euler update of the model (12) with the relaxation solution (14) at some arbitrarily small (but numerically reasonable) time step. Define $\delta\hat{t} \equiv (1 \times 10^{-3})\Delta t$. We may then write

$$Y_v(\delta\hat{t}) = Y_{v,0} - \delta\hat{t} \underbrace{\frac{1}{V} \sum_i A_i h_{m,i}(Y_{v,0} - Y_{l,i})}_{M} = Y_{eq} + (Y_{v,0} - Y_{eq}) \exp(-\omega \delta\hat{t}) \tag{15}$$

Solving for the time constant yields

$$\omega = -\frac{1}{\delta\hat{t}} \ln\left(1 - \frac{\delta\hat{t} M}{Y_{v,0} - Y_{eq}}\right) \tag{16}$$

which, with $\delta\hat{t}$ sufficiently small, is a positive number with units of s^{-1}.

With a closed form solution for the gas phase vapor fraction we can obtain an analytical solution to Eq. (1). The droplet mass as a function of time is

$$m(t) = \left(m_0^{1/3} + \frac{\beta}{3\omega}\left[1 - \exp(-\omega t)\right]\right)^3 \quad ; \quad \beta = \rho\chi h_m(Y_{v,0} - Y_{l,0}) \quad ; \quad \chi = 4\pi\left(\frac{3}{4\pi\rho_w}\right)^{2/3} \tag{17}$$

Note that χ comes from expressing the area of a drop with mass m as $A = \chi m^{2/3}$. The factor β may be thought of as the rate of mass transfer independent of the droplet mass.

The solution (17) is a cubic (see Fig. 5) and the mass becomes zero when t is

$$t_{m=0} = -\frac{1}{\omega} \ln\left(1 + \frac{3\omega m_0^{1/3}}{\beta}\right) \tag{18}$$

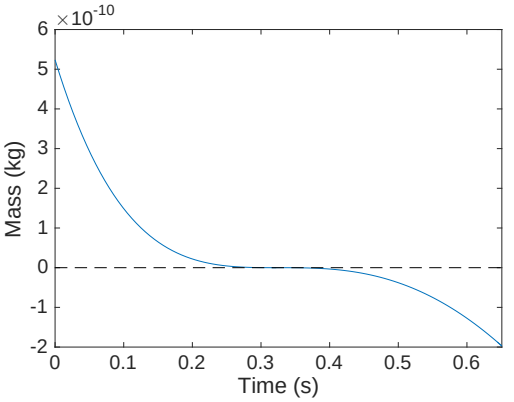

Fig. 5. Droplet mass solution for arbitrary parameter values ($m_0 = 5.3 \times 10^{-10}$, $\omega = 1$, $\beta = -0.0087$). For these parameters, the time to zero mass is $t_{m=0} = 0.3254$.

If the natural log argument is ≤ 0, this means the droplet does not fully evaporate.

Assume the gas phase temperature decays to equilibrium at the same rate as the mass.

$$T_g(t) = T_{eq} + (T_{g,0} - T_{eq})\exp(-\omega t) \tag{19}$$

The most difficult part of this integration is the droplet temperature. Based on the assumed solution (predictor) for the gas phase temperature, Eq. (19), the droplet temperature ODE may be rewritten as

$$\frac{\mathrm{d}T}{\mathrm{d}t} = m^{-1/3}\frac{\chi h}{c_{p,l}}([T_{g,0} - T_{eq}]\exp(-\omega t) + [T_{eq} - T]) + m^{-1}\frac{\dot{q}_r}{c_{p,l}} + m^{-1/3}\frac{\beta h_v}{c_{p,l}}\exp(-\omega t)$$

$$= F(t)T + G(t) \tag{20}$$

where

$$F(t) = -m^{-1/3}\frac{\chi h}{c_{p,l}} = \frac{-\chi h/c_{p,l}}{(m_0^{1/3} + \frac{\beta}{3\omega}[1 - \exp(-\omega t)])} \tag{21}$$

$$G(t) = \frac{\left(\frac{\chi h}{c_{p,l}}[T_{g,0} - T_{eq}] + \frac{\beta h_v}{c_{p,l}}\right)\exp(-\omega t) + \frac{\chi h}{c_{p,l}}T_{eq}}{(m_0^{1/3} + \frac{\beta}{3\omega}[1 - \exp(-\omega t)])} + \frac{\frac{\dot{q}_r}{c_{p,l}}}{(m_0^{1/3} + \frac{\beta}{3\omega}[1 - \exp(-\omega t)])^3} \tag{22}$$

A Crank-Nicolson scheme can be used to solve for the droplet temperature. This scheme is stable. However, it does not respect the equilibrium temperature. Overshoots and undershoots are avoided by setting the temperature to the equilibrium temperature when necessary.

The Crank-Nicolson scheme is

$$\frac{T^{n+1} - T^n}{\Delta t} = F(t^{n+\frac{1}{2}})\left(\frac{T^{n+1} + T^n}{2}\right) + G(t^{n+\frac{1}{2}}) \tag{23}$$

which leads to

$$T^{n+1} = \frac{T^n\left[1 + \frac{\Delta t F(t^{n+\frac{1}{2}})}{2}\right] + \Delta t\, G(t^{n+\frac{1}{2}})}{\left[1 - \frac{\Delta t F(t^{n+\frac{1}{2}})}{2}\right]} \tag{24}$$

where $t^{n+\frac{1}{2}} \equiv \frac{1}{2}(t^{n+1} - t^n)$. This scheme is stable because $F < 0$.

With the gas phase water vapor mass fraction determined as $Y_v(\Delta t)$, via Eq. (14), and individual droplet temperatures determined by Eq. (24), the gas phase temperature may be obtained from a simple energy balance. In practice, the appropriate source terms are accumulated and passed to the gas phase energy equation, which in FDS forms the velocity divergence constraint [4].

B Development of the Implicit Solution

In this appendix, we consider evaporation of a single drop in a computational cell away from the wall. Hence, our goal is to develop a solution for (a) the cell water vapor mass fraction Y_v, (b) the cell gas phase temperature T_g, and (c) the temperature of the ith droplet T_i. The inclusion of convective heat transfer to a wall surface cell is straight-forward. Details are provided in the FDS Technical Reference Guide [4].

The ODEs to be integrated are, respectively, the change in cell water vapor mass fraction, the change in the droplet temperature, and the change in the cell gas phase temperature:

$$\rho V \frac{\mathrm{d}Y_v}{\mathrm{d}t} = -\frac{\mathrm{d}m_i}{\mathrm{d}t} \tag{25}$$

$$m_i c_i \frac{\mathrm{d}T_i}{\mathrm{d}t} = A_g h_g (T_g - T_i) + \frac{\mathrm{d}m_i}{\mathrm{d}t} h_v + \dot{q}_r \tag{26}$$

$$m_g c_g \frac{\mathrm{d}T_g}{\mathrm{d}t} = -A_g h_g (T_g - T_i) + \frac{\mathrm{d}m_i}{\mathrm{d}t} (h_v + h_l) \tag{27}$$

Below we will consider the time integration for a single substep in the evaporation routine, which updates the local computational cell from time t^n to $t^n + \Delta t^n$. Usually, $\Delta t^n = \Delta t_{\mathrm{LES}}$. However, it is possible that subtimesteps may be required to prevent spurious mass and temperature overshoots. In what follows, unless otherwise specified RHS quantities are evaluated at the beginning of the substep, t^n (hence the designation "semi-implicit" method). This limits the stability range of the method (since the method is not fully implicit it is not unconditionally stable), but it greatly simplifies the solution procedure.

To begin the development, we expanded Eq. (25) with the mass loss rate (to be determined) evaluated at the midpoint of the time interval:

$$Y_v^{n+1} = Y_v^n - \frac{\Delta t^n}{\rho V} \left(\frac{\mathrm{d}m_i}{\mathrm{d}t} \right)^{n+\frac{1}{2}} \tag{28}$$

Substituting Eq. 28 into a Crank-Nicolson expansion of Eq. (1) we have

$$\begin{aligned} \left(\frac{\mathrm{d}m_i}{\mathrm{d}t} \right)^{n+1/2} &= -\frac{A_g h_{m,i} \rho}{2} \left(Y_{l,i}^{n+1} + Y_{l,i}^n - Y_v^{n+1} - Y_v^n \right) \\ &= -\frac{A_g h_{m,i} \rho}{2} \left(Y_{l,i}^{n+1} + Y_{l,i}^n - Y_v^n + \frac{\Delta t^n}{\rho V} \frac{\mathrm{d}m_i}{\mathrm{d}t} - Y_v^n \right) \\ &= -\frac{A_g h_{m,i} \rho}{2} \left[\frac{Y_{l,i}^{n+1} + Y_{l,i}^n - 2Y_v^n}{1 + \frac{\Delta t^n A_g h_{m,i}}{2V}} \right] \end{aligned} \tag{29}$$

Next, we find an approximation for the droplet surface equilibrium mass fraction $Y_{l,i}^{n+1}$ via the expansion

$$Y_{l,i}^{n+1} = Y_{l,i}^n + \left(\frac{\mathrm{d}Y_l}{\mathrm{d}T} \right)_i (T_i^{n+1} - T_i^n) \tag{30}$$

The derivative is determined from a chain rule expansion:

$$\left(\frac{\mathrm{d}Y_l}{\mathrm{d}T}\right)_i = \left(\frac{\mathrm{d}Y_l}{\mathrm{d}X_l}\right)\left(\frac{\mathrm{d}X_l}{\mathrm{d}T}\right)_i \tag{31}$$

The water vapor mole fraction on the surface of the droplet is determined from the Clausius-Clapeyron equation:

$$X_{v,l} = \exp\left[\frac{h_v W_v}{R}\left(\frac{1}{T_b} - \frac{1}{T_i}\right)\right] \tag{32}$$

For a binary mixture in air, the relationship between the vapor mass and mole fractions is given by

$$Y_{v,l} = \frac{X_{v,l}}{X_{v,l}(1 - W_a/W_v) + W_a/W_v} \tag{33}$$

Differentiating Eqs. (32) and (33) and substituting into (31) yields

$$\left(\frac{\mathrm{d}Y_l}{\mathrm{d}T}\right)_i = \frac{W_a/W_v}{\left(X_{l,i}(1 - W_a/W_v) + (W_a/W_v)\right)^2}\,\frac{h_v W_v}{R T_i^2}\exp\left[\frac{h_v W_v}{R}\left(\frac{1}{T_b} - \frac{1}{T_i}\right)\right] \tag{34}$$

Using (34) in (30), subsequently (30) in (29), and then (29) in (26) and (27), leaves two equations with two unknowns, T_i^{n+1} and T_g^{n+1}, to be solved simultaneously. As previously noted, unless otherwise indicated, all RHS quantities are evaluated at the beginning of the substep, t^n.

$$T_i^{n+1} = T_i^n + \frac{\Delta t^n}{m_i c_i}\left[A_g h_g\left(\frac{T_g^{n+1} + T_g^n}{2} - \frac{T_i^{n+1} + T_i^n}{2}\right) - \frac{A_g h_{m,i}\rho\left(Y_{l,i}^n + \frac{1}{2}\left(\frac{\mathrm{d}Y_l}{\mathrm{d}T}\right)_i\left(T_i^{n+1} - T_i^n\right) - Y_v^n\right)}{1 + \frac{\Delta t^n A_g h_{m,i}}{2V}} h_v + \dot{q}_r\right] \tag{35}$$

$$T_g^{n+1} = T_g^n + \frac{\Delta t^n A_g}{m_g c_g}\left[-h_g\left(\frac{T_g^{n+1} + T_g^n}{2} - \frac{T_i^{n+1} + T_i^n}{2}\right) + \frac{h_{m,i}\rho\left(Y_{l,i}^n + \frac{1}{2}\left(\frac{\mathrm{d}Y_l}{\mathrm{d}T}\right)_i\left(T_i^{n+1} - T_i^n\right) - Y_v^n\right)}{1 + \frac{\Delta t^n A_g h_{m,i}}{2V}}(h_v + h_l)\right] \tag{36}$$

Finally, the updated cell water vapor mass fraction, Y_v^{n+1}, may be found using (30) in (29), and then (29) in (28).

$$Y_v^{n+1} = Y_v^n + \frac{\Delta t^n}{\rho V}\frac{A_g h_{m,i}\rho}{2}\left[\frac{2Y_{l,i}^n + \left(\frac{\mathrm{d}Y_l}{\mathrm{d}T}\right)_i\left(T_i^{n+1} - T_i^n\right) - 2Y_v^n}{1 + \frac{\Delta t^n A_g h_{m,i}}{2V}}\right] \tag{37}$$

Special Cases

There are several special situations to consider. If the cell is on a surface and the droplets have impacted the surface then an additional heat transfer term with a wall temperature T_w is needed. The system of equations becomes 3×3, which complicates the algebra but the solution is nevertheless straightforward.

When the droplet completely evaporates, T_i^{n+1} is obviously undefined. In this case, a check is performed to ensure that the net heat transfer from the gas (and wall if present) does not exceed the energy required to evaporate the drop.

If the droplet temperature has increased over the boiling point (there is no inherent process in the method that prevents this), additional mass is evaporated to lower the temperature to the boiling point.

If the end state is supersaturated or if there is an unusually large change in droplet or gas temperature, then the timestep is subdivided and the droplet solution is repeated.